ACS Photonics

Article

pubs.acs.org/journal/apchd5

Color Separation through Spectrally-Selective Optical Funneling

Dimitrios L. Sounas and Andrea Alù*

Department of Electrical and Computer Engineering, The University of Texas at Austin, Austin, Texas 78712, United States

ABSTRACT: We present the concept and a basic design for a free-space color sorter, which can efficiently separate different spectral components of an optical beam. The structure is based on a resonant cavity formed between a metallic wall and a stack of partially reflecting screens. Such a cavity supports multiple leaky-wave resonances, which enable spectrally selective funneling of the incident beam through apertures in the metallic wall. The apertures are coupled to resonators with different resonance frequencies that allow separating different spectral components of the beam. The proposed concept can potentially overcome the efficiency limitations of color filter arrays, with important consequences in the design of fast and efficient spectral imaging systems.

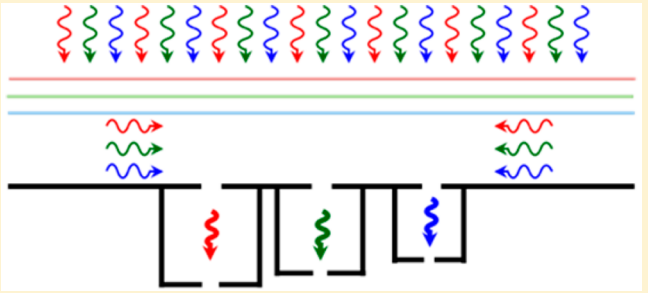

KEYWORDS: *color sorting, funneling, extraordinary optical transmission, leaky-wave antenna, optical nanodevices*

Color vision in the human eye relies on the wavelength sensitivity of our light receptors. On the other hand, artificial photodetectors are usually insensitive to different wavelengths, and for this reason, color cameras rely on filter arrays, which allow transmission of different wavelengths at different positions in space. A famous example is the Bayer filter,[1] whose unit cell is divided into four equal regions, one for transmission of red light, one for blue light and two for green light. The individual filters in a color-filter array are usually realized through layers of dyes with color-dependent transmission characteristics.[2] Plasmonic metasurfaces have also recently received significant attention in this context because of their small size and tunability characteristics.[3−6] However, despite their simplicity, color-filter arrays suffer from limited efficiency, since they reject the largest part of the incident signal. For example, a Bayer filter transmits only 25, 50, and 25% of the impinging red, green, and blue light, respectively. Overcoming this fundamental limitation is essential for improving the sensitivity of color sensors and cameras, but it requires a completely different approach than the one followed in conventional color-filter arrays. A possible solution toward this direction is based on diffractive filter arrays and optical signal postprocessing techniques,[7] but it involves computational overhead compared to purely analog approaches. It is clear that developing an analog device that can efficiently separate different spectral components of an optical beam is of large significance. Such an approach should necessarily be based on routing the different spectral components of light to different regions in space, similar to the routing of the different spectral components of a signal in an optical waveguide to different output optical waveguides through a wavelength-division demultiplexer.[8,9]

Toward this direction, extraordinary optical transmission (EOT)[10,11] offers a possible solution. EOT refers to the dramatic increase in the power transmitted through a subwavelength aperture in a metallic wall when the aperture is appropriately coupled to a resonance. The resonance essentially enhances the near field of the aperture and enables funneling of a significant part of the incident power through the aperture, well beyond ray optics expectations.[12−15] EOT has attracted significant attention both for its interesting physics and for its numerous applications in sensing, microscopy, and power harvesting. Different types of structures have so far been shown to exhibit EOT, including plasmonic gratings,[10] metamaterial slabs,[16,17] and slots supporting Fabry−Perot resonances.[18−20]

Due to its resonant nature, EOT is an inherently narrowband effect, which is a useful property for the separation of different spectral components of an optical signal. For example, by bringing gratings with different periodicities next to each other, it is possible to funnel different spectral components of impinging light through different apertures. Although such structures do not provide any efficiency improvement compared to a conventional color filter array, they allow reducing the size of photodetectors with important advantages in terms of speed. The transmission efficiency can be improved by partially overlapping different gratings,[21] although such an approach is limited by the fact that this overlap reduces the overall grating efficiency. Efficiency improvement can also be achieved by bringing subwavelength slots of different lengths next to each other,[22] however, only for beams with a width smaller than the wavelength. In a different context, color sorting has also been reported in arrays of plasmonic particles that focus impinging light at different points in space,[23−25] however, without any specific results about the efficiency of such systems.

Here, we present a structure that can separate different spectral components of optical beams without any fundamental

Received: December 16, 2015
Published: March 2, 2016

DOI: 10.1021/acsphotonics.5b00723
ACS Photonics 2016, 3, 620−626

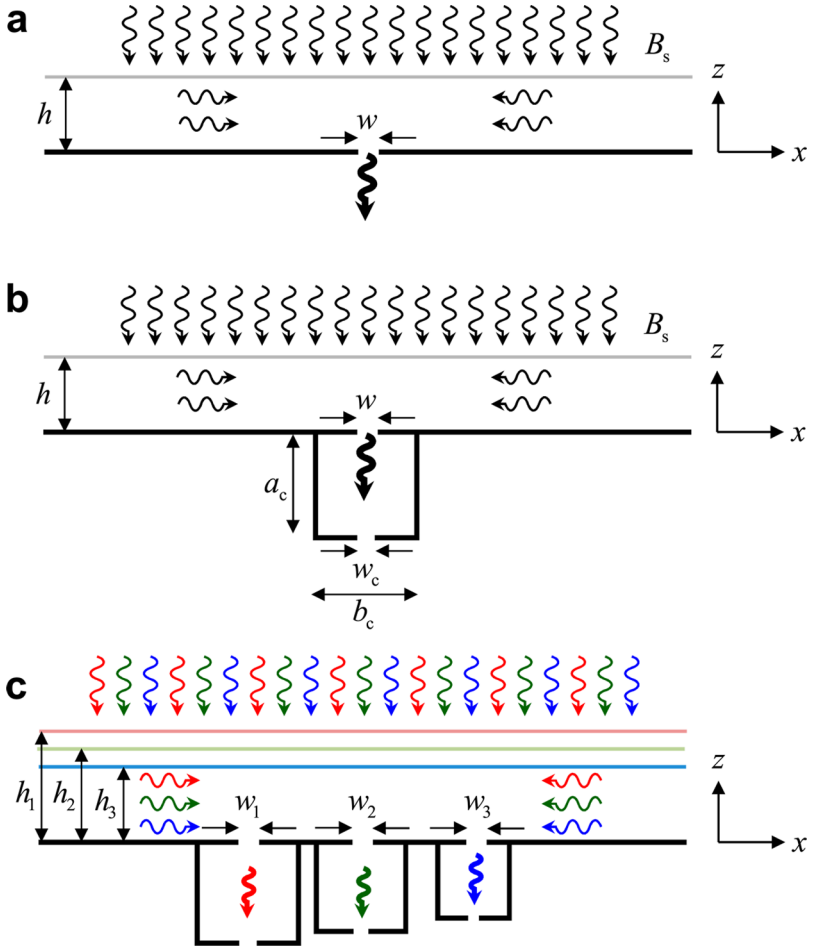

Figure 1. Separation of the spectral components of an optical beam in free space. (a) Funneling of a single spectral component of an optical beam through a small aperture. The structure consists of a metallic plane, where the aperture is located, and a partially reflecting screen at distance h. The screen is purely reactive with a susceptance B_s. Funneling is the result of the excitation of a leaky-wave resonance between the metallic plane and the screen. (b) Coupling of the structure in panel a to a resonant cavity for achieving conjugate matching at the aperture and maximizing the funneling efficiency. (c) Funneling and spatial separation of multiple spectral components (here three) of an optical beam. The metallic plane is covered with multiple partially reflecting screens. Each one of them supports a leaky-wave resonance at one of the funneled spectral components. Rectangular cavities with different resonance frequencies are coupled to apertures at the metallic plane for separation of the spectral components.

limitation in terms of peak efficiency or beamwidth. The proposed device is inspired by leaky-wave antennas (LWA) consisting of partially reflecting screens on top of perfectly electric conducting (PEC) planes.[14] Such structures support leaky wave resonances over areas much larger than the wavelength and can dramatically increase the directivity of sources placed between the ground plane and the screen. Due to reciprocity, if the source is replaced by a subwavelength aperture in the ground plane, as in Figure 1a, the same leaky-wave mechanism funnels a significant amount of power through the aperture, proportional to the antenna directivity in transmitting mode. Since our final goal is the separation of different spectral components of an impinging signal, we propose to cover the metal plane with a stack of partially reflecting screens at different distances, as in Figure 1c, so that multiple leaky-wave resonances can be excited at the desired frequencies, and consequently, multiple spectral components can be funneled through the aperture. Spatial splitting of the different spectral components collected by the LWA may be achieved by coupling the LWA to cavities with different resonant frequencies, as shown in the same figure. The cavities also allow achieving conjugate matching between the LWA and the aperture, which is necessary to maximize the received power. In the following, we provide more details about the proposed setup, and present preliminary designs based on metallic planes coupled to lossless partially reflecting screens. For simplicity, the analysis here focuses on the 2D scenario, i.e., on structures that are invariant along the y-axis with electric fields polarized along the y-axis. All numerical results have been obtained through full-wave simulations with the commercial software Comsol Multiphysics.

RESULTS AND DISCUSSION

A parameter which is typically used to characterize the receiving properties of an antenna is its effective area A_{eff}, defined as $A_{eff} = W_r/P_{inc}$, where W_r is the received power and P_{inc} is the incident power density. For structures invariant along a particular direction (here, the y-direction) and in the absence of material loss, the effective area is related to the directivity D of the antenna as $A_{eff} = D\lambda/2\pi$,[26] showing that A_{eff} and D become maximum under the same conditions. For the LWA in Figure 1a, D is maximum when[27]

$$\mathrm{Im}\{k_{x,\mathrm{LW}}\} = \sqrt{3}\,\mathrm{Re}\{k_{x,\mathrm{LW}}\} \quad (1)$$

DOI: 10.1021/acsphotonics.5b00723
ACS Photonics 2016, 3, 620−626

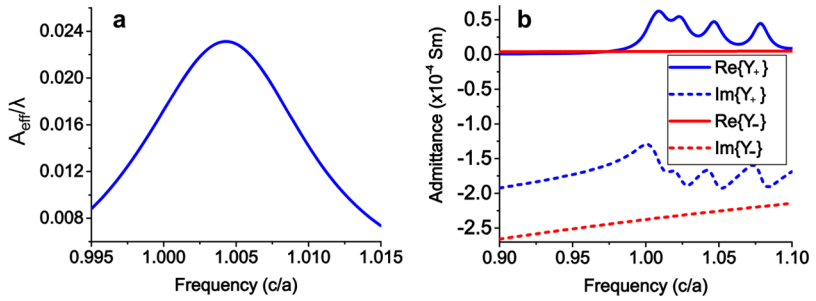

Figure 2. Power funneling of a single spectral component via the structure in Figure 1a. (a) Effective aperture of the structure in Figure 1a vs frequency for $B_s = 6.94Y_0$, $h = 0.52a$, and aperture width $w = 0.1a$. (b) Input admittance of the aperture vs frequency. The computational domain is terminated with PMC boundary conditions along the x-axis, which for a periodic structure, as here, are equivalent to periodic boundary conditions. Then, the resonant peaks in the aperture admittance are the result of coupling between adjacent unit cells.

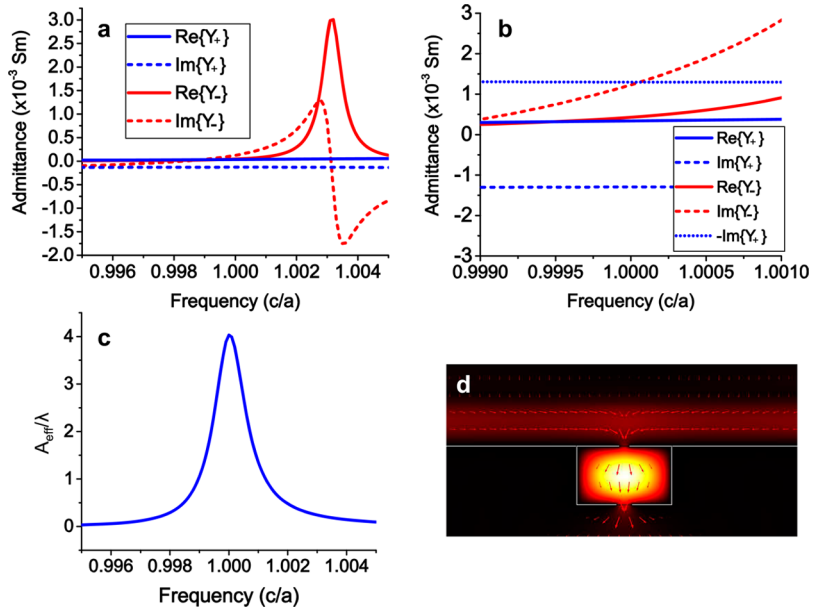

Figure 3. Power funneling of a single spectral component via the structure in Figure 1a, when the aperture is coupled to a resonant cavity, as the ones in Figure 1b. (a) Input admittance of the aperture versus frequency. The parameters of the LWA (B_s, h, and w) are the same as in Figure 2. The dimensions of the cavity along the x- and z-axes are $a_c = 0.939a$ and $b_c = 0.567a$, respectively. The width of the aperture at the bottom wall of the cavity is $w_c = 0.153a$. (b) Snapshot of panel close to the center frequency. (c) Effective area vs frequency. (d) Electric field distribution and power flow at the center frequency.

where $k_{x,LW}$ is the transverse wavenumber of the leaky mode supported by the structure.[28] The corresponding values of D and A_{eff} read

$$D_{max} = 3.15\frac{k_0}{\mathrm{Im}\{k_{x,LW}\}},\quad A_{eff,max} = \frac{2\pi}{\mathrm{Im}\{k_{x,LW}\}} \tag{2}$$

Equation 2 allows determining $\mathrm{Im}\{k_{x,LW}\}$, and from eq 1, also $\mathrm{Re}\{k_{x,LW}\}$, in order to achieve a specified A_{eff} of interest. Knowing $k_{x,LW}$, the parameters of the structure, including the screen susceptance B_s, and the distance of the screen from the ground plane h, may be derived from the transverse resonance equation

$$Y + iB_s - iY\ \cot(k_{z,LW}h) = 0 \tag{3}$$

where $k_{z,LW} = (k_0^2 - k_{x,Lw}^2)^{1/2}$ is the wavenumber along the direction normal to the screen, k_0 is the wavenumber in free space, $Y = Y_0 k_{z,LW}/k_0$ is the admittance for fields parallel to the screen, and $Y_0 = 1/(120\pi)$ S is the free-space admittance.

Based on this analysis, we designed a LWA, as in Figure 1a, with effective aperture $A_{eff} = 4a$, where a is a reference length equal to the free-space wavelength λ_0 at the center frequency f_0. Substituting this value into eqs 2 and 3 yields $B_s = 6.94Y_0$ and $h = 0.52a$. For these design parameters and an aperture width $w = 0.1a$, Figure 2a shows A_{eff} versus frequency, as calculated through full-wave simulations. The thickness of all metallic walls is taken as $0.01a$ and, for simplicity, the temporal dispersion of B_s is neglected, which is a valid approximation for a leaky mode with a small decay rate and, therefore, a large Q-factor. In any case, the dispersion of B_s affects the bandwidth but not the effective aperture at resonance, in which we are mostly interested. The dispersion of B_s will be fully considered in the analysis of the multiple-screen scenario of Figure 1c.

Quite surprisingly, the maximum value of A_{eff} is much smaller than the one for which the structure was designed ($0.023a$ instead of $4a$), and it happens at a frequency larger than the frequency for which the structure is expected to have maximum effective area ($1.004f_0$ instead of f_0). This behavior is the result of the fact that conjugate matching is not satisfied at the aperture, as required in order for $A_{eff} = D\lambda/2\pi$ and,

DOI: 10.1021/acsphotonics.5b00723
ACS Photonics 2016, 3, 620−626

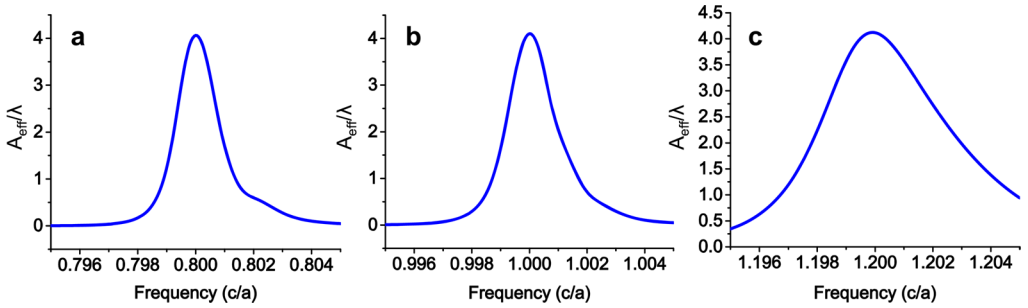

Figure 4. Power funneling of multiple spectral components via the structure in Figure 1c, but with a single aperture and a single cavity, as in Figure 1b. The frequencies of funneled components are $f_1 = 0.8c/a$, $f_2 = c/a$, and $f_2 = 1.2c/a$. The resonance frequencies of the partially reflective screens are $f_{r1} = 0.787c/a$, $f_{r2} = 0.978c/a$, $f_{r3} = 1.11c/a$, and the corresponding distances from the bottom wall $h_1 = 0.47a$, $h_2 = 0.41a$, and $h_3 = 0.38a$. (a) Effective area for an aperture at the bottom wall of the LWA with width $w = 0.16a$ and cavity parameters $a_c = 1.15a$, $b_c = 0.71a$, $w_c = 0.255a$. (b) Effective area for an aperture at the bottom wall of the LWA with width $w = 0.128a$ and cavity parameters $a_c = 0.93a$, $b_c = 0.57a$, $w_c = 0.2a$. (c) Effective area for an aperture at the bottom wall of the LWA with width $w = 0.107a$ and cavity parameters $a_c = 0.77a$, $b_c = 0.48a$, $w_c = 0.16a$.

subsequently, eq 2 to hold. This fact can be better understood through the general equation

$$A_{\text{eff}} = D\frac{\lambda}{2\pi}\frac{4\text{Re}\{Y_+\}\text{Re}\{Y_-\}}{|Y_+ + Y_-|^2} \tag{4}$$

where Y_+ and Y_- are the aperture admittances toward its upper and lower side, respectively, defined as

$$Y_+ = \frac{2\int_{S_a}\mathbf{S}_+^*\cdot\hat{z}\,dS}{|E_0|^2} \tag{5}$$

$$Y_- = -\frac{2\int_{S_a}\mathbf{S}_-^*\cdot\hat{z}\,dS}{|E_0|^2} \tag{6}$$

In the above equations, $\mathbf{S}_+$ and $\mathbf{S}_-$ is the complex Poynting vectors on the upper and lower side of the aperture when it is excited by an electric field $E_y(x) = E_0\sqrt{1-(2x/w)^2}$, which is a very good approximation of the actual field in a subwavelength aperture.[29] It can be seen from eq 4 that A_{eff} becomes maximum and equal to $D\lambda/2\pi$ for $Y_+ = Y_-^*$ ($\text{Re}\{Y_+\} = \text{Re}\{Y_-\}$ and $\text{Im}\{Y_+\} = -\text{Im}\{Y_-\}$), that is, under conjugate matching of the upper and lower sides of the aperture.

The admittances Y_+ and Y_- are shown versus frequency in Figure 2b. It can be seen from this figure that, although $\text{Re}\{Y_+\} = \text{Re}\{Y_-\}$ at frequency $0.97c/a$, $\text{Im}\{Y_+\}$ is always different from $-\text{Im}\{Y_-\}$ and, therefore, conjugate matching is not satisfied. It is worth observing that $\text{Im}\{Y_-\}$ takes large negative values, showing that the aperture stores a large amount of inductive energy. The leaky wave reduces this inductive energy, as it can be seen from the smaller negative values of $\text{Im}\{Y_+\}$ compared to $\text{Im}\{Y_-\}$, but it cannot fully compensate it to achieve conjugate matching. An additional element is necessary to compensate the inductive energy of the aperture, which can be achieved with a cavity at frequencies slightly below its resonance, where the cavity can store large amounts of capacitive energy. This is seen in Figure 3a, which shows Y_+ and Y_- when such a cavity is attached to the bottom side of the ground plane, as in Figure 1b. The parameters of the cavity, provided in the caption of the figure, were selected to provide conjugate matching at the center frequency f_0 (see also Figure 3b, which is a zoom of Figure 2c close to f_0). The slight difference between the frequencies where conjugate matching conditions $\text{Re}\{Y_+\} = \text{Re}\{Y_-\}$ and $\text{Im}\{Y_+\} = \text{Im}\{Y_-\}$ are satisfied is attributed to the fact that the electric field distribution assumed in eqs 5 and 6 is only an approximation of the actual field distribution in the gap. The effective area for the conjugate-matched system of the LWA and the cavity is presented in Figure 3c, showing that it takes a maximum value of $4a$ at the center frequency f_0, in accordance with the design specifications. Notice that the resonance bandwidth is smaller than in Figure 2a due to the resonant cavity. Finally, Figure 3d presents the field profile and power flow at f_0, clearly showing the funneling mechanism.

The separation of different spectral components of an incident optical beam requires a structure that supports multiple leaky-wave resonances, a functionality that can be achieved with the structure in Figure 1c, consisting of a ground plane and multiple partially reflecting screens at different distances from the ground plane. Ideally, each screen should support, together with the ground plane, a single leaky-wave resonance. This feature can be achieved if each screen is reflective at a particular leaky wave resonance, while being almost transparent at all other resonances. It is evident that in such a case the screens need to be dispersive. The simplest dispersion model that satisfies this requirement is a lossless Lorentzian model for the screen susceptance:

$$B_s = \frac{2Y_0}{Q}\frac{\omega\omega_0}{-\omega^2+\omega_0^2} \tag{7}$$

where ω_0 is the resonance frequency and Q is the corresponding quality factor. ω_0 needs to be close to the frequency of the leaky-wave resonance, so that B_s is large and the screen is highly reflective at this resonance, as required to obtain a small $k_{x,\text{LW}}$ and a large A_{eff}. At the same time, for appropriately large Q, B_s is small, far from ω_0, and the screen is almost transparent at the other leaky-wave resonances. The Q-factor required to satisfy this requirement is very large for the frequency separation between leaky-wave resonances considered here, imposing restrictions on the bandwidth of the entire structure. This requirement can be relaxed if we allow each screen to have a small but non-negligible effect on the resonances of the others. Then, instead of eq 3, the screen susceptances need to satisfy the modified transverse-resonance equation

$$Y_{\text{in}} + Y = 0 \tag{8}$$

where Y_{in} is the input admittance of the structure from the top side of the outermost screen. Y_{in} effectively incorporates the

DOI: 10.1021/acsphotonics.5b00723
ACS Photonics 2016, 3, 620−626

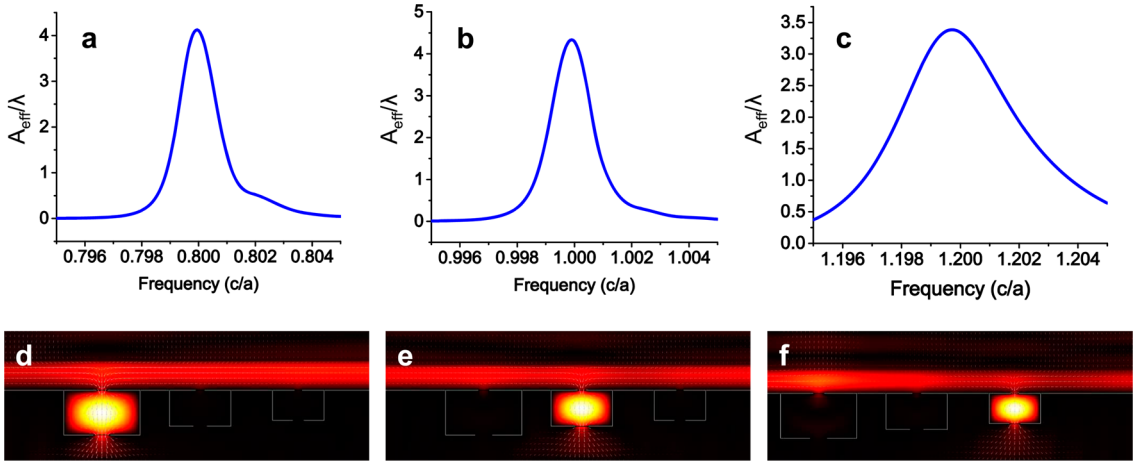

Figure 5. Power funneling of multiple spectral components via the structure in Figure 1c, with the same parameters for the LWA and the cavities as in Figure 4. (a) Effective area for transmission through the first aperture. (b) Effective area for transmission through the second aperture. (c) Effective area for transmission through the third aperture. (d) Electric field distribution and power flow at f_1. (e) Electric field distribution and power flow at f_2. (f) Electric field distribution and power flow at f_3.

effect of all screens. By solving eq 8, we can determine the optimal resonance frequencies of the screens, and the distances of the screens from the ground plane.

Based on the above considerations, we designed a structure that funnels the frequencies $f_1 = 0.8c/a$, $f_2 = c/a$, and $f_3 = 1.2c/a$, with effective apertures $A_{1,\text{eff}} = 4\lambda_1$, $A_{2,\text{eff}} = 4\lambda_2$, and $A_{3,\text{eff}} = 4\lambda_3$, respectively, where λ_i is the wavelength at frequency f_i. The Q-factor of the screens was selected as 4.5, which was found to lead to maximum funneling bandwidth. The small Q-factor for the partially reflective screen is a very important advantage of the proposed approach since it may allow the optical realization of such surfaces with plasmonic metasurfaces. For example, a periodic metasurface consisting of resonant plasmonic dipoles can provide low and high transmission at and far from the dipole resonance, thus satisfying the requirements for the partially reflecting screens in the proposed devices. Yet, even for so low Q-factor, loss will affect the efficiency of the structure, reducing the amount of received power. This problem can be overcome by using dielectric metasurfaces, which are based on dielectric resonant particles, such as silicon nanoparticles, and provide similar response to plasmonic metasurfaces, however, without their loss problems.[31] The calculated values for the resonance frequencies of the screens and the corresponding distances from the ground plane are $f_{r1} = 0.787c/a$, $h_1 = 0.47a$, $f_{r2} = 0.978c/a$, $h_2 = 0.41a$, $f_{r3} = 1.11c/a$, and $h_3 = 0.38a$. The aperture has variable width $0.128\lambda_i$, depending of the operation frequency f_i, and is coupled to a cavity, as in Figure 1b, with dimensions, as given in the caption of Figure 4, so that conjugate matching is achieved at f_i. Note that the cavity dimensions are different for different frequencies. Figure 4 presents the effective area versus frequency, as derived from full-wave simulations. A_{eff} takes its maximum values $4\lambda_1$, $4\lambda_2$, and $4\lambda_3$ at frequencies f_1, f_2, and f_3, respectively, as designed.

The three cavities described above can now be used for spatial separation of frequencies f_1, f_2, and f_3 if they are simultaneously attached to the bottom wall of the antenna, as in Figure 1c. The frequency separation is made possible by the fact that the input admittance of each cavity far from its resonance is very small, as it can be seen in Figure 3a, essentially making the cavity an open circuit far from its resonance. Figure 5 presents numerical results for the effective area, the field profile, and the power flow for the structure described above. It can be seen that the collected power by the LWA at frequencies f_1, f_2, and f_3 is transmitted through different cavities, as desired. Notice that A_{eff} is equal to $4\lambda_1$ and $4\lambda_2$ at frequencies f_1 and f_2, respectively, in accordance with the design specifications for the LWA. On the other hand, A_{eff} at f_3 is equal to $3.4\lambda_3$, slightly smaller than its specified value, because f_3 is close to the second-order resonance of the first cavity, resulting in a finite input admittance for this cavity and subsequently allowing a small but non-negligible part of the collected incident power at f_3 to be transmitted through this cavity.

CONCLUSIONS

The structure presented here bears interesting connections with integrated wavelength division multiplexers based on photonic crystals, as in ref 9. Also, these devices consist of a cavity that collects different spectral components from an input channel and additional cavities that discriminate these components. However, there is a fundamental difference between an integrated multiplexer and the structure presented here: the input channel in an integrated multiplexer is usually a single-mode photonic waveguide with well-defined boundaries and width usually in the order of half the wavelength. This fact significantly relaxes the requirements in terms of the Q-factor for the collecting cavity. Even a broad-band, single-mode cavity is sufficient to collect multiple spectral components of an input signal with very large efficiencies. On the other hand, the input channel in the free-space scenario investigated here is a plane wave with much larger extent. Collecting power from a plane wave over distances larger than the wavelength necessarily requires the excitation of a leaky-wave resonance. The amount of power that can be collected by such resonances is inversely proportional to their Q-factor, showing that, in order to be able to collect a significant amount of power, a large Q-factor is necessary. It is clear that separating the spectral components of light in free-space is a far more challenging task than in an integrated circuit, and it has significantly broader implications for imaging and energy harvesting.

The structures presented here are based on a PEC material, which may seem problematic for optical applications for which metals cannot be assumed ideal conductors. However, it is important to stress that such an approach has been followed to

DOI: 10.1021/acsphotonics.5b00723
ACS Photonics 2016, 3, 620−626

simplify the analysis, and it is not related to any fundamental limitation of the proposed devices. The important property of a PEC ground plane is that it provides precise control over the location where the collected power at the top side of the antenna is funneled at its bottom side through the aperture on the ground plane. Such a functionality can also be provided by metals at optical frequencies, with the only difference that, due to the finite penetration depth of electromagnetic fields in metals at such frequencies, the thickness of the ground plane needs to be adequately large so that waves can be transmitted through an aperture on the ground plane but not through the bulk of the material. The finite penetration depth of fields in the metallic ground plane at optical frequencies will also affect the frequency of the leaky-wave resonance and the aperture dimensions that maximize the funneling capability of the structure, but such effects can be precisely considered in the analytical model presented in the previous section. These facts show the generality of the proposed approach and its potential for applications at different frequency ranges.

The analyzed structures were designed to provide optimum response when excited with *y*-polarized waves. A funneling effect is also expected for *x*-polarized waves, but in a suboptimal way, since the aperture dimensions are not optimized for this particular polarization. The fact that the analyzed structures can be optimized only for a particular polarization is related to their extreme anisotropy in the $x-y$ plane: the aperture on the ground plane is subwavelength along the *x*-axis, but infinite along the *y*-axis. Such a problem will not exist in a 3D scenario based on symmetric circular apertures on the ground plane. In such a case, rotational symmetry will lead to the same efficiency for *x*- and *y*-polarized waves, thus, removing the polarization limitations of the designs discussed in the present paper.

Although the proposed structures exhibit peak efficiency much larger than conventional color filter arrays, it may be argued that, since this phenomenon occurs over a narrow bandwidth, the overall efficiency of the system, which is proportional to the product BW × A_{eff} of bandwidth and peak effective area, will be much smaller than for a color filter array. For example, the systems proposed here exhibit BW × $A_{eff} \approx$ 0.004, which is much smaller than for color-filter arrays. Our approach may be therefore attractive for applications that involve the detection of narrow spectral lines, such as molecular spectroscopy in chemistry and astrophysics. In such a case, the bandwidth in BW × A_{eff} is determined by the spectral lines that we want to detect and the broad bandwidth of a color filter array has negligible effect on the efficiency. On the other hand, the efficiency can be significantly enhanced by increasing A_{eff}, as in the devices we propose here.

One of the main challenges in an optical realization of the proposed structure is represented by material loss, which is expected to impose a trade-off between A_{eff} and efficiency. A possible way to compensate for this trade-off is by considering periodic arrangements of the basic structure in Figure 1c with a period equal to the value of A_{eff}, for which efficiency is within acceptable levels. In such a case, the collected incident power at *N* different frequencies is transmitted through *N* different arrays of apertures, instead of *N* different apertures, as in Figures 1c and 5. Such a structure would resemble recently proposed structures with absorption capabilities at multiple frequencies, which are constructed by embedding multiple resonant elements with different resonant frequencies inside the unit cell of a periodic array.[30] Furthermore, it should be noted that the overall loss of the structure can be significantly reduced by employing dielectric gratings, multilayers, or recently proposed dielectric metasurfaces,[31] to realize the partially reflecting screens and the ground plane. The above considerations show that there are no fundamental limitations regarding the realization and functionality of the proposed structure, opening a new venue toward the design of efficient color sorters with applications in spectral imaging devices.

METHODS

The simulations were performed with the commercial software Comsol Multiphysics based on the finite element method. The computational domain was terminated with perfectly matched layers along the *z*-axis and perfect-magnetic-conductor (PMC) boundary conditions along the *x*-axis. For a symmetric structure with respect to the *z*-axis, *y*-polarized electric field, and normal incidence, as for the structures analyzed here, the PMC boundary conditions are equivalent to periodic boundary conditions. The width of the computational domain along the *x*-axis was selected as 11λ in order to minimize coupling between adjacent unit cells through the leaky mode. The decay length of this mode is proportional to $1/\mathrm{Im}\{k_{x,\mathrm{LW}}\}$ and it increases as frequency increases (the leaky mode becomes more confined as frequency increases). Therefore, although the selected width may be enough to minimize coupling at the design frequency (the frequency where a maximum effective area is desired), it may not be at higher frequencies, resulting in the admittance resonances in Figure 2b. However, in addition to the fact that these resonances are outside the band of interest, their effect on A_{eff} is negligible, since the aperture admittances at these resonances are very far from the conjugate matching condition.

AUTHOR INFORMATION

Corresponding Author

*E-mail: alu@mail.utexas.edu.

Notes

The authors declare no competing financial interest.

ACKNOWLEDGMENTS

This work was supported by AFOSR with Grant No. FA9550-13-1-0204 and the NSF CAREER Award No. ECCS 0953311.

REFERENCES

(1) Bayer, B. E. Color imaging array. U.S. Patent 3,971,065, 1976.

(2) Lukac, R.; Plataniotis, K. N. Color filter arrays: design and performance analysis. *IEEE Trans. Consum. Electron.* **2005**, *51*, 1260–1267.

(3) Lee, H.-S.; Yoon, Y.-T.; Lee, S.-L.; Kim, S.-H.; Lee, K.-D. Color filter based on a subwavelength patterned metal grating. *Opt. Express* **2007**, *15*, 15457–15463.

(4) Diest, K.; Dionne, J. A.; Spain, M.; Atwater, H. A. Tunable color filters based on metal-insulator-metal resonators. *Nano Lett.* **2009**, *9*, 2579–2583.

(5) Xu, T.; Wu, Y.-K.; Luo, X.; Guo, L. J. Plasmonic nanoresonators for high-resolution colour filtering and spectral imaging. *Nat. Commun.* **2010**, *1*, 59.

(6) Haïdar, R.; Vincent, G.; Collin, S.; Bardou, N.; Guérineau, N.; Deschamps, J.; Pelouard, J.-L. Free-standing subwavelength metallic gratings for snapshot multispectral imaging. *Appl. Phys. Lett.* **2010**, *96*, 221104.

(7) Wang, P.; Menon, R. Ultra-high-sensitivity color imaging via a transparent diffractive-filter array and computational optics. *Optica* **2015**, *2*, 933–939.

DOI: 10.1021/acsphotonics.5b00723
ACS Photonics 2016, 3, 620–626

(8) Saleh, B. E. A.; Teich, M. C. *Fundamentals of Photonics*, 2nd Ed.; John Wiley and Sons, 2007.
(9) Jin, C.; Fan, S.; Han, S.; Zhang, D. Reflectionless multichannel wavelength demultiplexer in a transmission resonator configuration. *IEEE J. Quantum Electron.* **2003**, *39*, 160−165.
(10) Genet, C.; Ebbesen, T. W. Light in tiny holes. *Nature* **2007**, *445*, 39−46.
(11) Garcia-Vidal, F. J.; Martin-Moreno, L.; Ebbesen, T. W.; Kuipers, L. Light passing through subwavelength apertures. *Rev. Mod. Phys.* **2010**, *82*, 729−787.
(12) Oliner, A. A.; Jackson, D. R. Leaky surface-plasmon theory for dramatically enhanced transmission through a subwavelength aperture, Part I: Basic features. IEEE Antennas and Propagation Society International Symposium, Columbus, OH, U.S.A., June 22−27, 2003, IEEE: Piscataway, NJ, 2003.
(13) Jackson, D. R.; Zhao, T.; Williams, J. T.; Oliner, A. A. Leaky surface-plasmon theory for dramatically enhanced transmission through a sub-wavelength aperture, Part II: Leaky-wave antenna model. IEEE Antennas and Propagation Society International Symposium, Columbus, OH, U.S.A., June 22−27, 2003, IEEE: Piscataway, NJ, 2003.
(14) Jackson, D. R.; Burghignoli, P.; Lovat, G.; Capolino, F.; Chen, J.; Wilton, D. R.; Oliner, A. A. The fundamental physics of directive beaming at microwave and optical frequencies and the role of leaky waves. *Proc. IEEE* **2011**, *99*, 1780−1805.
(15) Pardo, F.; Bouchon, P.; Haïdar, R.; Pelouard, J.-L. Light funneling mechanism explained by magnetoelectric interference. *Phys. Rev. Lett.* **2011**, *107*, 093902.
(16) Alù, A.; Bilotti, F.; Engheta, N.; Vegni, L. Metamaterial covers over a small aperture. *IEEE Trans. Antennas Propag.* **2006**, *54*, 1632−1643.
(17) Aydin, K.; Cakmak, A. O.; Sahin, L.; Li, Z.; Bilotti, F.; Vegni, L.; Ozbay, E. Split-ring-resonator-coupled enhanced transmission through a single subwavelength aperture. *Phys. Rev. Lett.* **2009**, *102*, 013904.
(18) Takakura, Y. Optical resonance in a narrow slit in a thick metallic screen. *Phys. Rev. Lett.* **2001**, *86*, 5601−5603.
(19) Garcia-Vidal, F.; Moreno, E.; Porto, J. A.; Martin-Moreno, L. Transmission of light through a single rectangular hole. *Phys. Rev. Lett.* **2005**, *95*, 103901.
(20) Merlin, R. Pinholes meet Fabry-Pérot: perfect and imperfect transmission of waves through small apertures. *Phys. Rev. X* **2012**, *2*, 031015.
(21) Laux, E.; Genet, C.; Skauli, T.; Ebbesen, T. W. Plasmonic photon sorters for spectral and polarimetric imaging. *Nat. Photonics* **2008**, *2*, 161−164.
(22) Büyükalp, Y.; Catrysse, P. B.; Shin, W.; Fan, S. Spectral light separator based on deep-subwavelength resonant apertures in a metallic film. *Appl. Phys. Lett.* **2014**, *105*, 011114.
(23) Tanemura, T.; Balram, K. C.; Ly-Gagnon, D.-S.; Wahl, P.; White, J. S.; Brongersma, M. L.; Miller, D. A. B. Multiple-wavelength focusing of surface plasmons with a nonperiodic nanoslit coupler. *Nano Lett.* **2011**, *11*, 2693−2698.
(24) Shegai, T.; Chen, S.; Miljković, V. D.; Zengin, G.; Johansson, P.; Käll, M. A bimetallic nanoantenna for directional colour sorting. *Nat. Commun.* **2011**, *2*, 481.
(25) Liu, J. S. Q.; Pala, R. A.; Afshinmanesh, F.; Cai, W.; Brongersma, M. L. A submicron plasmonic dichroic splitter. *Nat. Commun.* **2011**, *2*, 525.
(26) Balanis, C. A. *Antenna Theory: Analysis and Design*; John Wiley and Sons, 2005.
(27) See Supporting Information.
(28) Lovat, G.; Burghignoli, P.; Jackson, D. R. Fundamental properties and optimization of broadside radiation from uniform leaky-wave antennas. *IEEE Trans. Antennas Propag.* **2006**, *54*, 1442−1452.
(29) Harrington, R. F. *Time Harmonic Electromagnetic Fields*; John Wiley and Sons, 2001.
(30) Mann, S. A.; Garnett, E. C. Resonant nanophotonic spectrum splitting for ultrathin multijunction solar cells. *ACS Photonics* **2015**, *2*, 816−821.
(31) Wu, C.; Arju, N.; Kelp, G.; Fan, J. A.; Dominguez, J.; Gonzales, E.; Tutuc, E.; Brener, I.; Shvets, G. Spectrally selective chiral silicon metasurfaces based on infrared Fano resonances. *Nat. Commun.* **2014**, *5*, 3982.

DOI: 10.1021/acsphotonics.5b00723
ACS Photonics 2016, 3, 620−626